

Supplementary Material for

Ponatinib combined with rapamycin causes regression of murine Venous Malformation

Xian Li^{1*}, Yuqi Cai^{1*}, Jillian Goines^{1*}, Patricia Pastura², Lars Brichta³, Adam Lane⁴, Timothy D. Le Cras^{2,5}, Elisa Boscolo^{1,5#}

¹Divisions of Experimental Hematology and Cancer Biology, Cancer and Blood Disease Institute, Cincinnati Children's Hospital Medical Center, Cincinnati, Ohio, 45229 USA

² Division of Pulmonary Biology, Cincinnati Children's Hospital Medical Center, Cincinnati, Ohio, 45229 USA

³ Chemistry Rx- Compounding and Specialty Pharmacy, Philadelphia PA, 19107 USA

⁴Division of Bone Marrow Transplantation and Immune Deficiency, Cancer and Blood Disease Institute, Cincinnati Children's Hospital Medical Center, Cincinnati, Ohio, 45229 USA

⁵ Department of Pediatrics, University of Cincinnati College of Medicine, Cincinnati, OH

* These authors contributed equally to this work

Corresponding author: elisa.boscolo@cchmc.org

The PDF file includes:

Supplementary results, Supplementary Material and Methods.

Fig. I. Proliferation rates of HUVEC-TIE2-L914F (L914F) and VM-EC.

Fig. II. Specificity of ABL kinase inhibitors Ponatinib, Nilotinib and Bosutinib.

Fig. III. c-ABL and ARG knockdown prevents lumen enlargement in a 3D fibrin gel assay.

Fig. IV. Proliferation inhibition curves in HUVEC-TIE2-L914F treated with ABL kinase inhibitors combined with rapamycin.

Fig. V. Combination treatment with Ponatinib and rapamycin is effective in preventing VM murine lesion expansion.

Fig. VI. Comparison of different reduced dose combination treatments in the VM murine model.

Fig. VII. Effects of reduced dose combination treatment in the formation of VM lesions.

Fig. VIII. Ponatinib combined with rapamycin promotes lesion regression, even at reduced dose.

Fig. IX. Long-term combination treatment of Ponatinib with rapamycin in the murine VM model.

Fig. X. Topical rapamycin treatment prevents lesion rebound.

Fig. XI. Combination treatment with Ponatinib and rapamycin increases apoptosis.

Fig. XII. Combination treatment with Ponatinib and rapamycin reduces vascular area in a 3D fibrin gel assay.

Fig. XIII. Quantification of active signaling pathways in patient-derived VM-EC.

Fig. XIV. Combination treatment with Ponatinib and rapamycin reduces vascular area in a VM patient-derived xenograft model.

Fig. XV. Schematic model of combination therapy for the treatment of VM.

Table I. Cell-based drug screening assay results.

Table II. List of candidate drugs and IC₅₀ values.

Table III. Combination Index (CI) values.

Supplementary results:

Dose-ranging study of the combination treatment.

Based on a synergistic anti-proliferative effect *in vitro* (Suppl. fig. IV and Table III), it was reasonable to test combination of rapamycin and Ponatinib *in vivo*. After injection of HUVEC-TIE2-L914F cells, mice were treated with vehicle, rapamycin, Ponatinib or combination for 15 days. At day16 (Suppl. fig. V), in Ponatinib or rapamycin monotherapy groups, VM lesion size was smaller than vehicle and untreated mice. Moreover, VM lesion size was decreased after combination treatment when compared to vehicle or non-treatment but also when compared to Ponatinib or rapamycin monotherapy groups. Lesion weight was also lower in the combination group compared to the vehicle or Ponatinib groups (Suppl. fig. V). Analysis of the H&E staining in the lesion explants showed that the drug combination prevented HUVEC-TIE2-L914F cells to form enlarged lumen in VM lesions (Suppl. fig. V). There was a trend to decreased mouse weight in the combination group compared to vehicle group, which suggested this dose of combination treatment may induce some side effects (Suppl. fig. V). For this reason, we tested two different reduced dose combinations (RD1 Combo; 20mg/kg Ponatinib + 1mg/kg rapamycin and RD2 Combo; 10mg/kg Ponatinib + 0.5mg/kg rapamycin) in the VM murine model. As shown in Suppl. figs. VI and VI, lesion size of RD1 Combo was smaller than vehicle, Ponatinib or rapamycin group at day 16. Conversely, lesion size in RD2 Combo group was similar to Ponatinib alone. RD1 Combo treatment, but not RD2 Combo, induced notable reduction in lesion weight (Suppl. fig. VI) and vascular area compared to vehicle or monotherapy group (Suppl. figs. VI and VI). Furthermore, there was no difference in mouse weight between RD1 Combo or RD2 Combo treatment and vehicle groups (Suppl. fig. VI).

Drug combination inhibits formation of HUVEC-TIE2-L914F-derived VM.

To compare the efficacy of combination and reduced dose combination, mice were injected with HUVEC-TIE2-L914F cells and at the same time, given vehicle, Ponatinib (30mg/kg), rapamycin (2mg/kg), combination and RD Combo (20mg/kg Ponatinib + 1mg/kg rapamycin). After 15 days of treatment, lesion size and lesion weight in both the combination and RD Combo groups were smaller compared to monotherapy and vehicle treated groups (Suppl. fig. VII). H&E staining of lesion explants showed that both combination and RD Combo prevented vessel enlargement (Suppl. fig. VII). These results suggest that: 1-drug combination is more effective than monotherapy; 2-reduced dose drug combination achieved similar effect on lesion expansion inhibition. We next evaluated the efficacy of combination and RD1 Combo in inducing VM lesion regression (see manuscript Fig. 2 and Suppl. fig.VIII and IX).

Supplementary Material and Methods:

Apoptosis (cleaved caspase-3 staining)

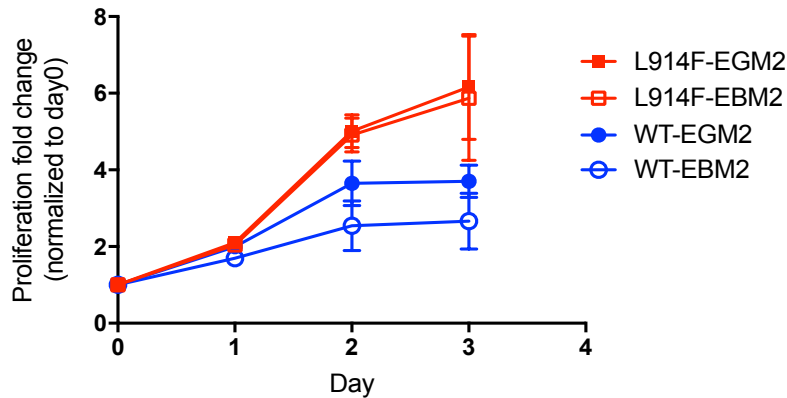
HUVEC-TIE2-L914F were seeded in Millicell® EZ SLIDE 4-well glass slides (EMD Millipore), and were treated by DMSO, Ponatinib, rapamycin or combination for 72 hours. Then slides were stained with AlexaFluor® 647 conjugated cleaved-caspase 3 (Cell signaling) to detect cell apoptosis. Nuclei were stained with 4',6- diamidino-2-phenylindole (DAPI).

VM patient-derived cell xenograft model

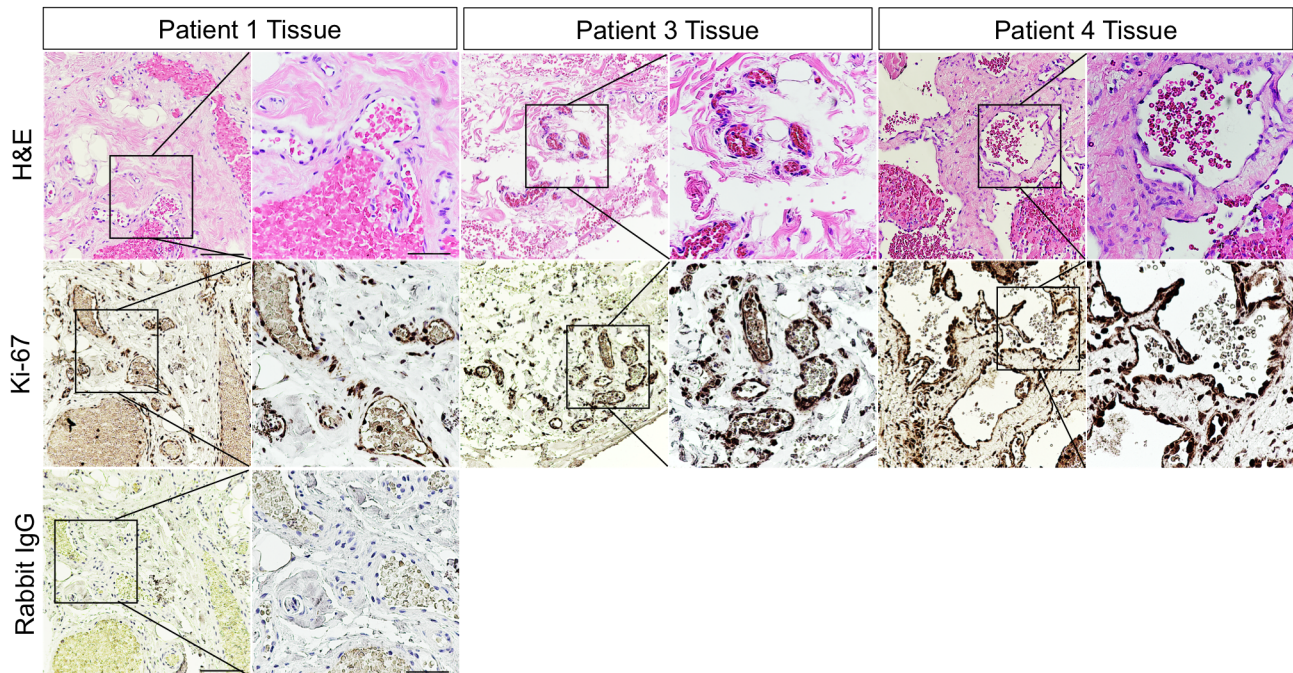
After cell expansion, 3.5×10^6 patient-derived VM-EC were suspended in Matrigel™ and injected subcutaneously (s.c.) on both flanks of 6-7 weeks old male athymic nu/nu mice. When most lesions turned red in appearance and average lesion size in each group exceeded 70 mm^2 , animals received oral gavage daily of 200µl vehicle (Citric buffer pH 2.5; 25mM – Ethanol 30% (v/v) solution), rapamycin (2mg/kg) or reduced combination (20mg/kg Ponatinib + 1mg/kg rapamycin) for 14 days. Size of lesions (mm^2) was measured with a caliper. Lesions were dissected, fixed in 10% formalin and processed for paraffin embedding. After Hematoxylin and Eosin (H&E) staining of paraffin sections, 5 images were taken randomly per section, then vessel density (Total vessels/lesion) was quantified with ImageJ software.

Supplementary Figures:

A

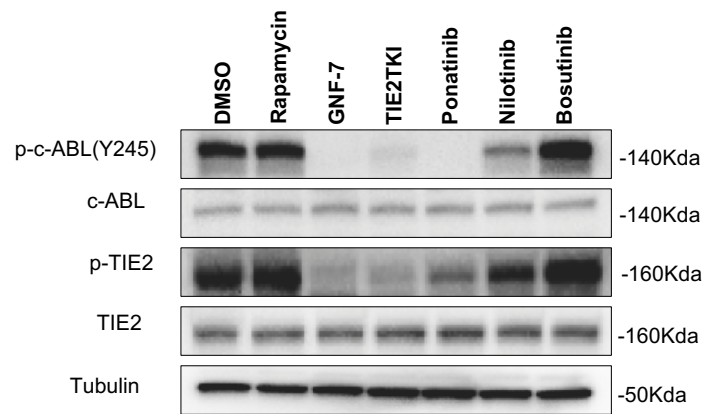


B

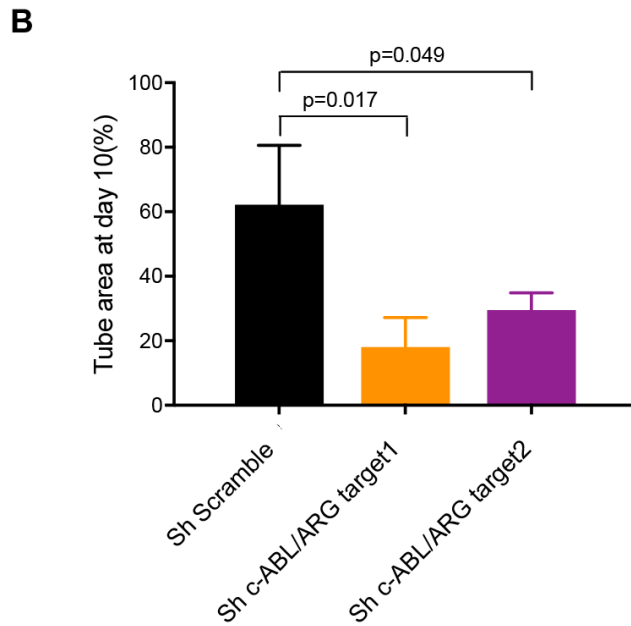
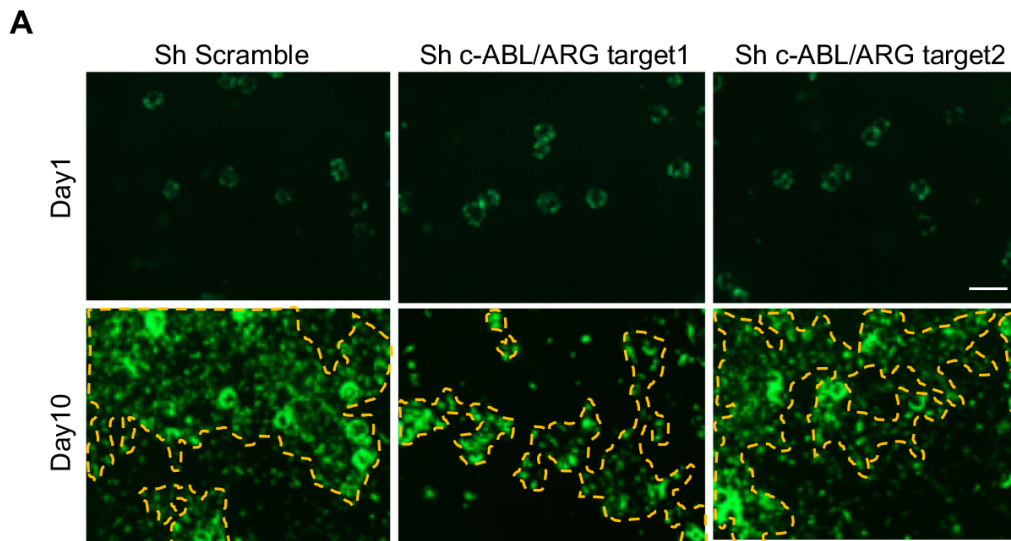


Supplemental figure I. Proliferation rates of HUVEC-TIE2-L914F (L914F) and VM-EC.

A. Cells were seeded at day -1 and fixed at day0, day1, day2 and day3 separately and OD values were read at 540 nm. Proliferation rate was normalized to day 0. EGM2: Endothelial Growth Factor Medium/20% FBS, EBM2: Endothelial Basal Medium (no growth factors). **B.** Patient tissue stained for hematoxylin and eosin (H&E) (top), Ki-67 (dark brown) (middle) and control rabbit IgG (bottom). Patient#1 and #3 tissue showed expression of the TIE2-L914F mutation. Scale bar: 100 μ m (left) and 50 μ m (right).

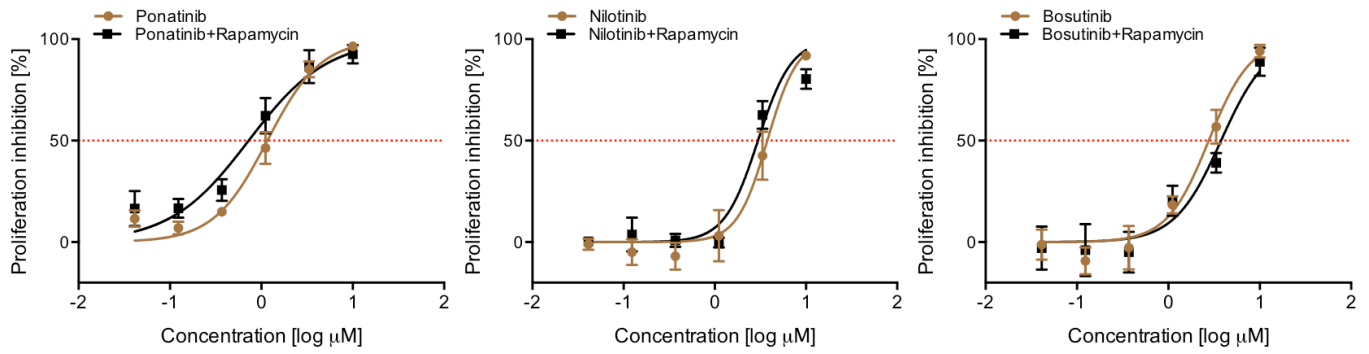


Supplemental figure II. Specificity of ABL kinase inhibitors Ponatinib, Nilotinib and Bosutinib. Western blotting analysis of HUVEC-TIE2-L914F with indicated antibodies. Cells were treated with DMSO (Control), rapamycin (15nM), GNF-7 (30nM), TIE2 tyrosine kinase inhibitor (TIE2-TKI) (10μM), Ponatinib (300nM), Nilotinib (10μM), or Bosutinib (10μM), for 1h.



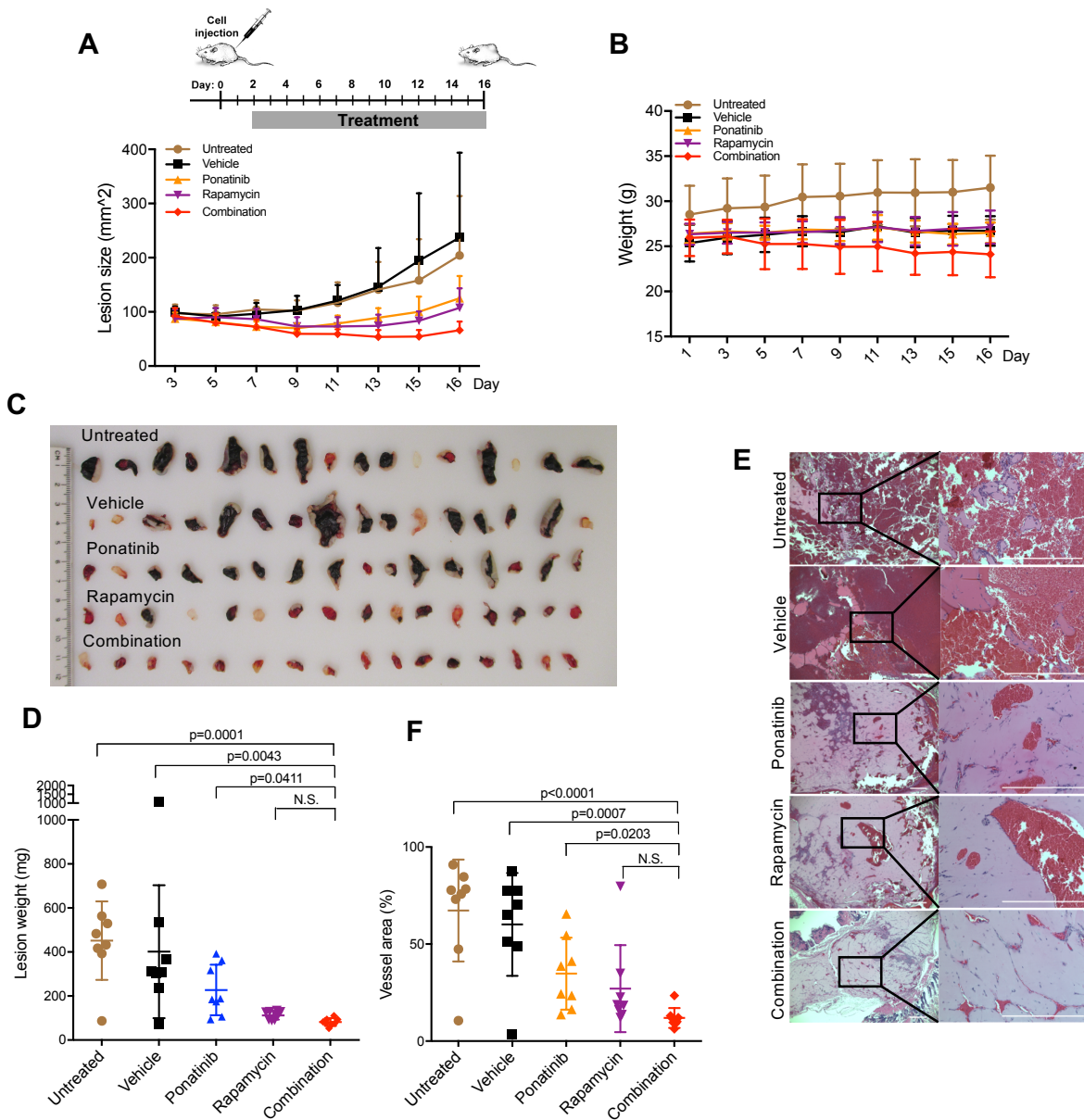
Supplemental figure III. c-ABL and ARG knockdown prevents lumen enlargement in a 3D fibrin gel assay.

A. Representative images of HUVEC-TIE2-L914F-GFP tube network formation taken on the same field at day 1 and day 10. Scale bar=200 μ m. **B.** Quantification of the tube area at day 10. Data expressed as mean \pm SD, n=3.



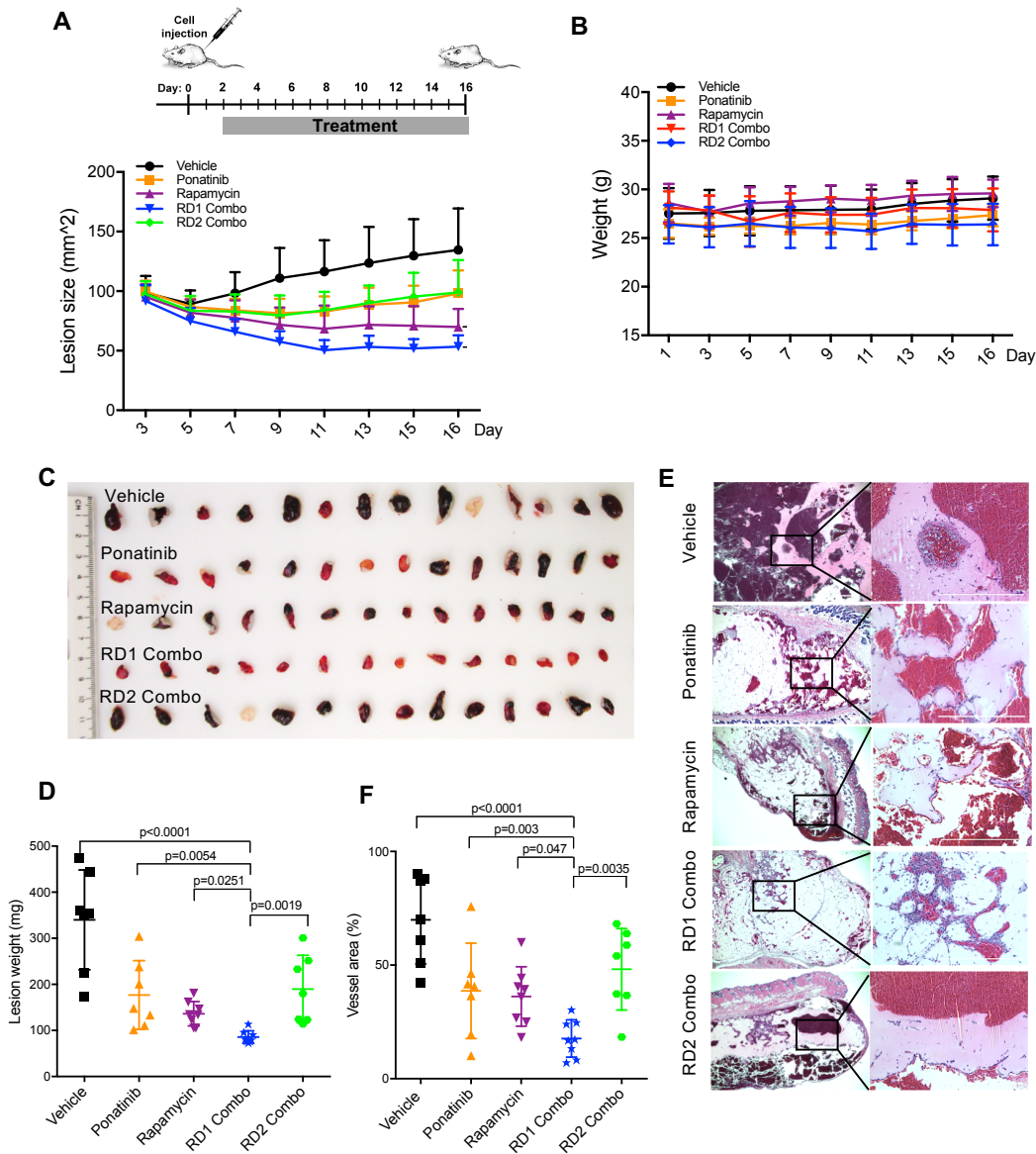
Supplemental figure IV. Proliferation inhibition curves in HUVEC-TIE2-L914F treated with ABL kinase inhibitors combined with rapamycin.

HUVEC-TIE2-L914F were treated with different concentrations (from 10μM to 0.03μM) of Ponatinib, Nilotinib or Bosutinib alone or in the presence of rapamycin at 10 nM for 72 h. Combination-rapamycin: rapamycin inhibition effect is deducted from the combination curve. Data expressed as mean ± SD, n=4.



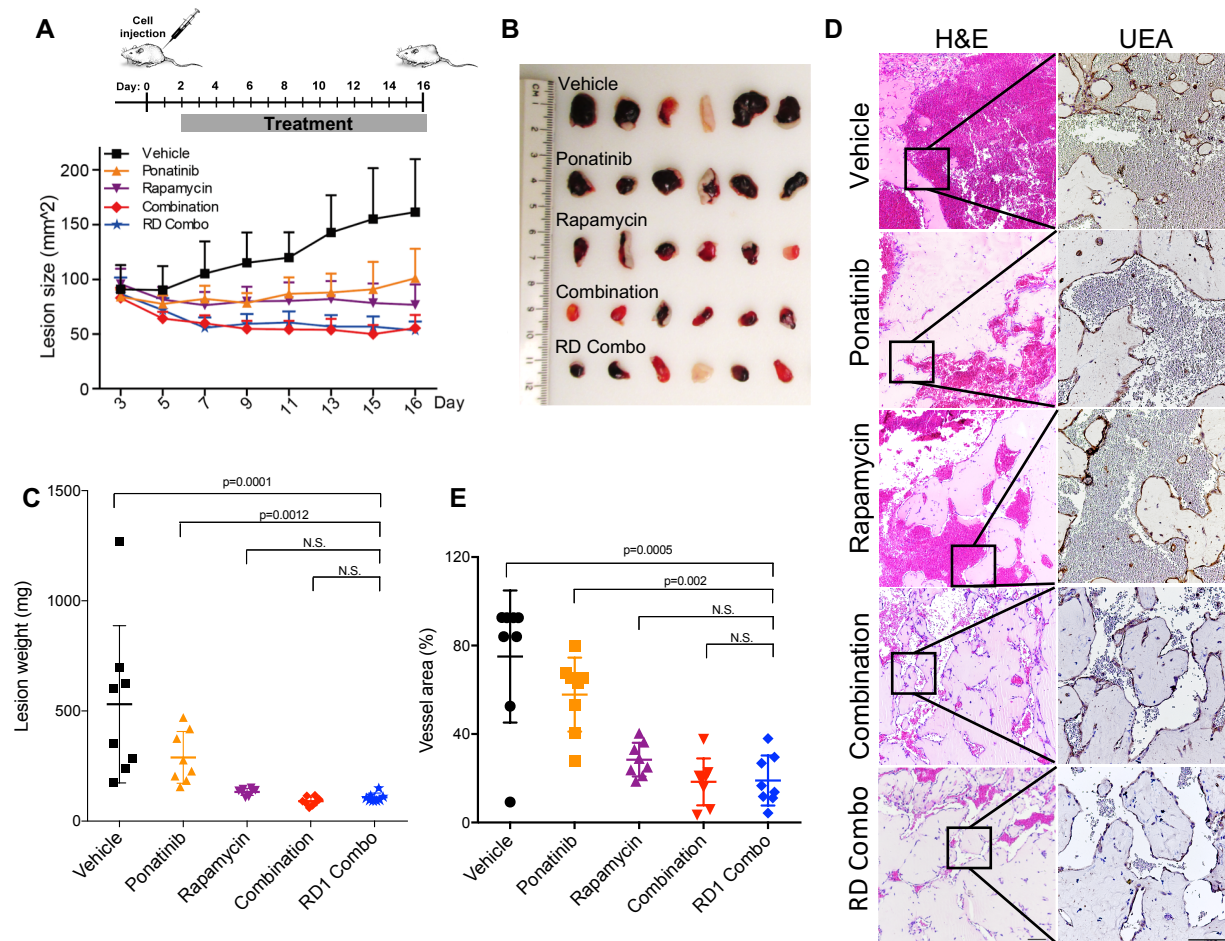
Supplemental figure V. Combination treatment with Ponatinib and rapamycin is effective in preventing VM murine lesion expansion.

A. HUVEC-TIE2-L914F injected nude mice were treated by oral gavage every day with vehicle, Ponatinib (30mg/kg), rapamycin (2mg/kg) or combination starting at day 1 for 15 days. Lesion size measured by caliper every 2 days until day16. Data expressed as mean \pm SD (n = 8 mice with 2 lesions/group). **B.** Mouse weight measured every 2 days until day16. Data expressed as mean \pm SD (n = 8 mice/group). **C.** Overview of lesions. **D.** Quantification of lesion weight. **E.** Representative H&E stained sections. Scale bar: 500 μ m. **F.** Quantification of vessel area. In D and F data expressed as average value for 2 lesions on each mouse, mean shown by horizontal bars, one-way Anova for multiple comparisons (n = 8 mice).



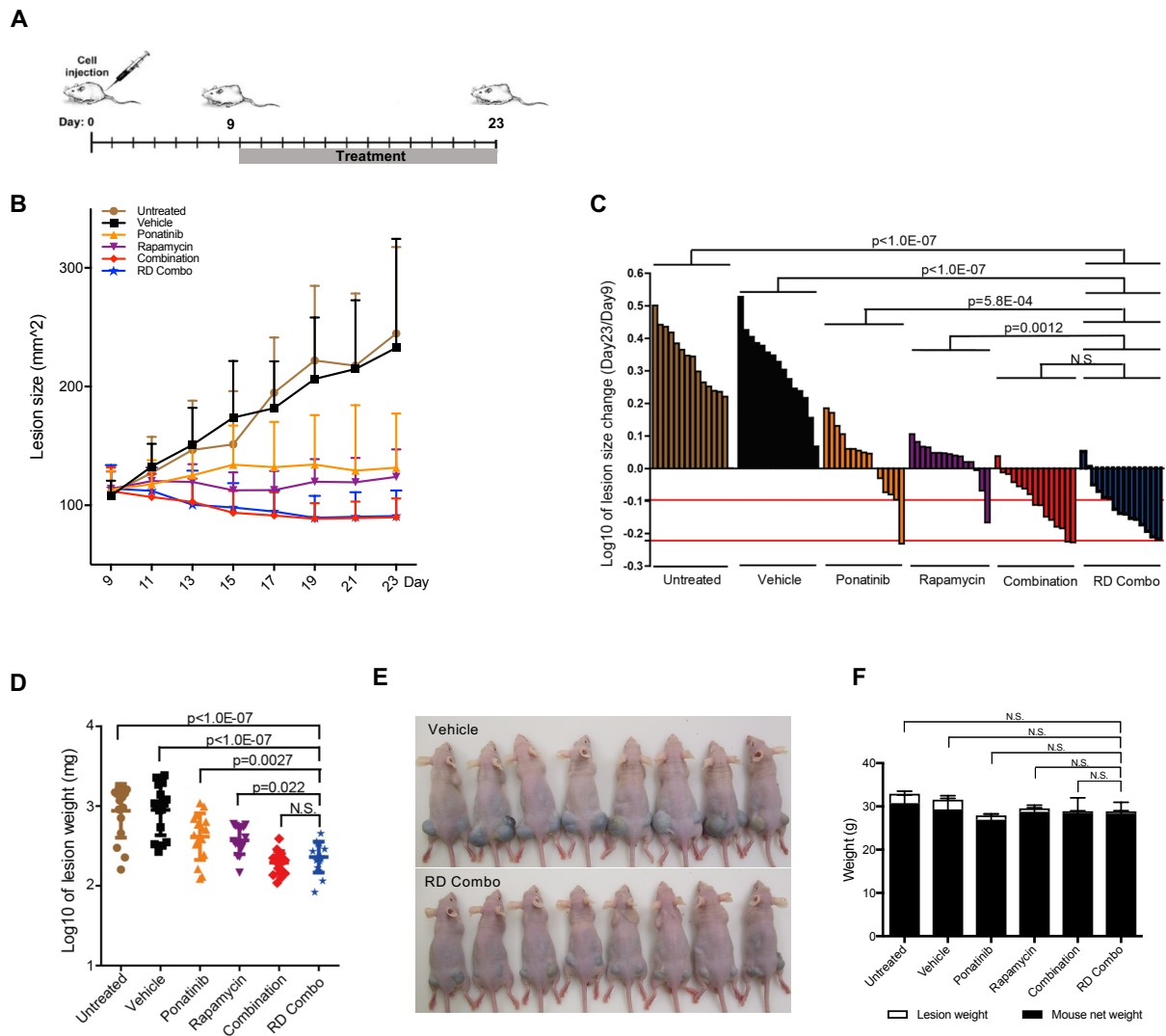
Supplemental figure VI. Comparison of different reduced dose combination treatments in the VM murine model.

A. HUVEC-TIE2-L914F injected mice were treated by oral gavage every day starting day 1 with vehicle, Ponatinib (30mg/kg), rapamycin (2mg/kg) or reduced dose 1 combination (RD1 Combo, Ponatinib 20mg/kg/day and rapamycin 1mg/kg) or reduced dose 2 combination (RD2 Combo, Ponatinib 10mg/kg/day and rapamycin 0.5mg/kg) for 15 days. Lesion size measured by caliper every 2 days until day 16. Data expressed as mean \pm SD (n = 8 mice with 2 lesions/group). **B.** Mouse weight measured every 2 days until day 16. Data expressed as mean \pm SD (n = 8 mice/group). **C.** Overview of lesions. **D.** Quantification of lesion weight. **E.** Representative H&E stained sections. Scale bar: 500 μ m. **F.** Quantification of vessel area. In D and F data expressed as average value for 2 lesions on each mouse, mean shown by horizontal bars, one-way Anova for multiple comparisons (n = 8 mice).



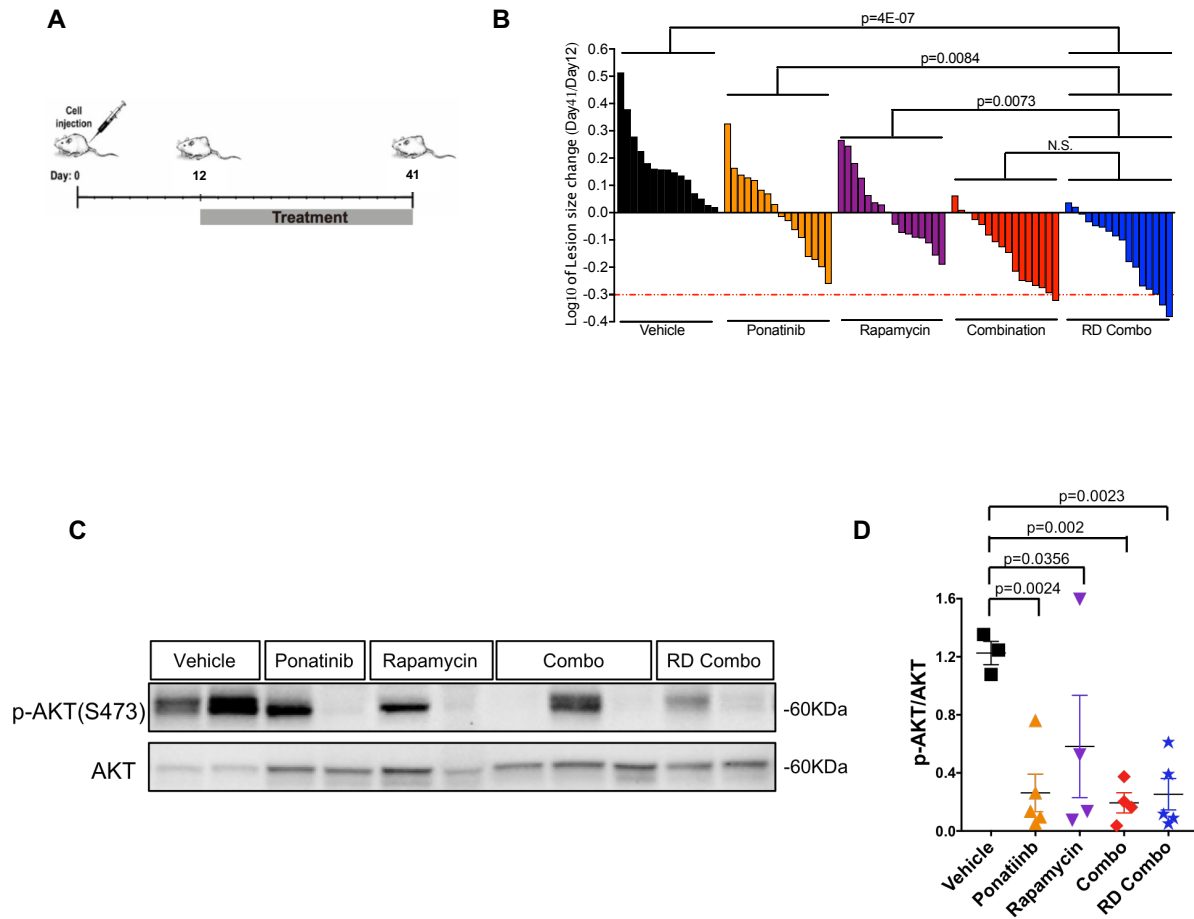
Supplemental figure VII. Effects of reduced dose combination treatment in the formation and expansion of VM lesions.

A. HUVEC-TIE2-L914F injected mice were treated by oral gavage daily from day 1 to day 15 with vehicle, Ponatinib (30mg/kg), rapamycin (2mg/kg), combination or reduced dose combination (RD Combo: Ponatinib 20mg/kg/day and rapamycin 1mg/kg). Lesions were measured by caliper every 2 days. Data expressed as mean \pm SD (n = 8 mice with 2 lesions/group). **B.** Representative images of lesions. **C.** Lesion weight. **D.** Representative H&E stained sections. Scale bar: 500 μ m. **E.** Quantification of vessel area. In C and E data expressed as average value for 2 lesions on each mouse, mean shown by horizontal bars, one-way Anova for multiple comparisons (n = 8 mice).



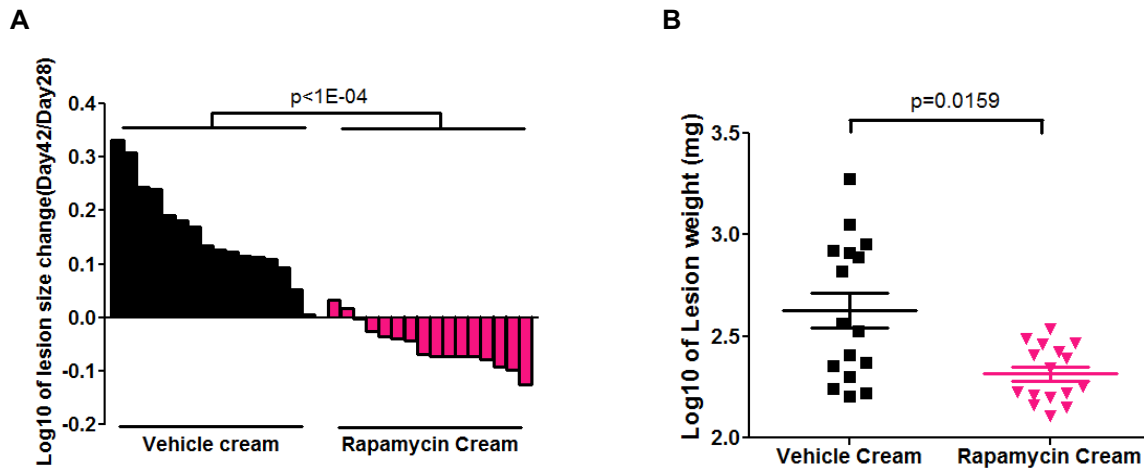
Supplemental figure VIII. Ponatinib combined with rapamycin promotes lesion regression, even at reduced dose.

A. Treatment scheme. When average VM lesion reached 110mm² (day 9), HUVEC-TIE2-L914F injected mice were treated daily by oral gavage with vehicle, Ponatinib(30mg/kg), rapamycin(2mg/kg), combination or reduced dose combination (RD Combo) (Ponatinib 20mg/kg/day and rapamycin 1mg/kg) for 14 days. **B.** Lesion size measured every 2 days. Data expressed as mean ± SD (n = 8 mice with 2 lesions/group). **C.** Waterfall plot of Log₁₀ of lesion size change (Day23/Day9). Data expressed as single value for each lesion, linear mixed model effect (n = 8 mice with 2 lesions/group). **D.** Log₁₀ of lesion weight. Data expressed as mean ± SD, linear mixed model effect (n = 8 mice with 2 lesions/group). **E.** Images of mice bearing lesions. **F.** Quantification of mouse body weight at day 23. In long-term experiments HUVEC TIE2-L914F formed very large VM lesions in untreated and vehicle groups compared to treated groups. Mouse and lesion weight were measured at day 23, then mouse net body weight was calculated by subtracting lesion weight from the total mouse weight. Mouse weight loss during the treatment was not noted. Data expressed as mean ± SD (n = 8 mice/group).



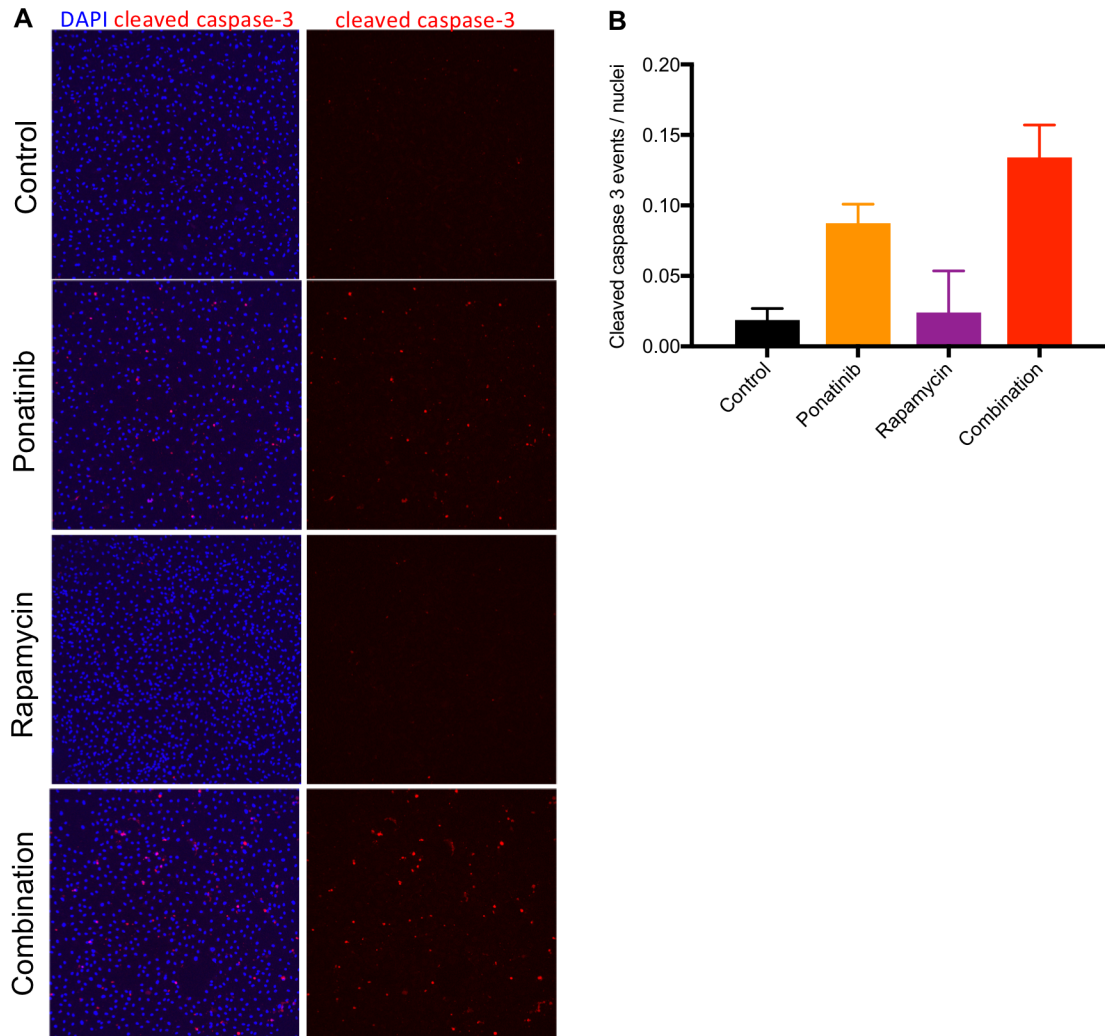
Supplemental figure IX. Long-term combination treatment of Ponatinib with rapamycin in the murine VM model.

A. Treatment scheme. When average VM lesion in each group reached 130mm² (day12), HUVEC TIE2-L914F injected mice were treated by oral gavage every day with vehicle, Ponatinib(30mg/kg), rapamycin(2mg/kg), combination or reduced dose combination (RD Combo) (Ponatinib 20mg/kg/day and rapamycin 1mg/kg) for 28 days. **B.** Waterfall plot of Log10 of lesion size change (Day41/Day12). Data expressed as single value for each lesion, linear mixed effect model (n = 8 mice with 2 lesions/group, one lesion in vehicle group was broken at day34 and is not shown). **C.** Representative immunoblot for p-AKT(Ser473) and total AKT in VM lesions. **D.** Quantification of p-AKT/AKT ratio from n=3-5 lesions/group, one-way Anova for multiple comparisons.



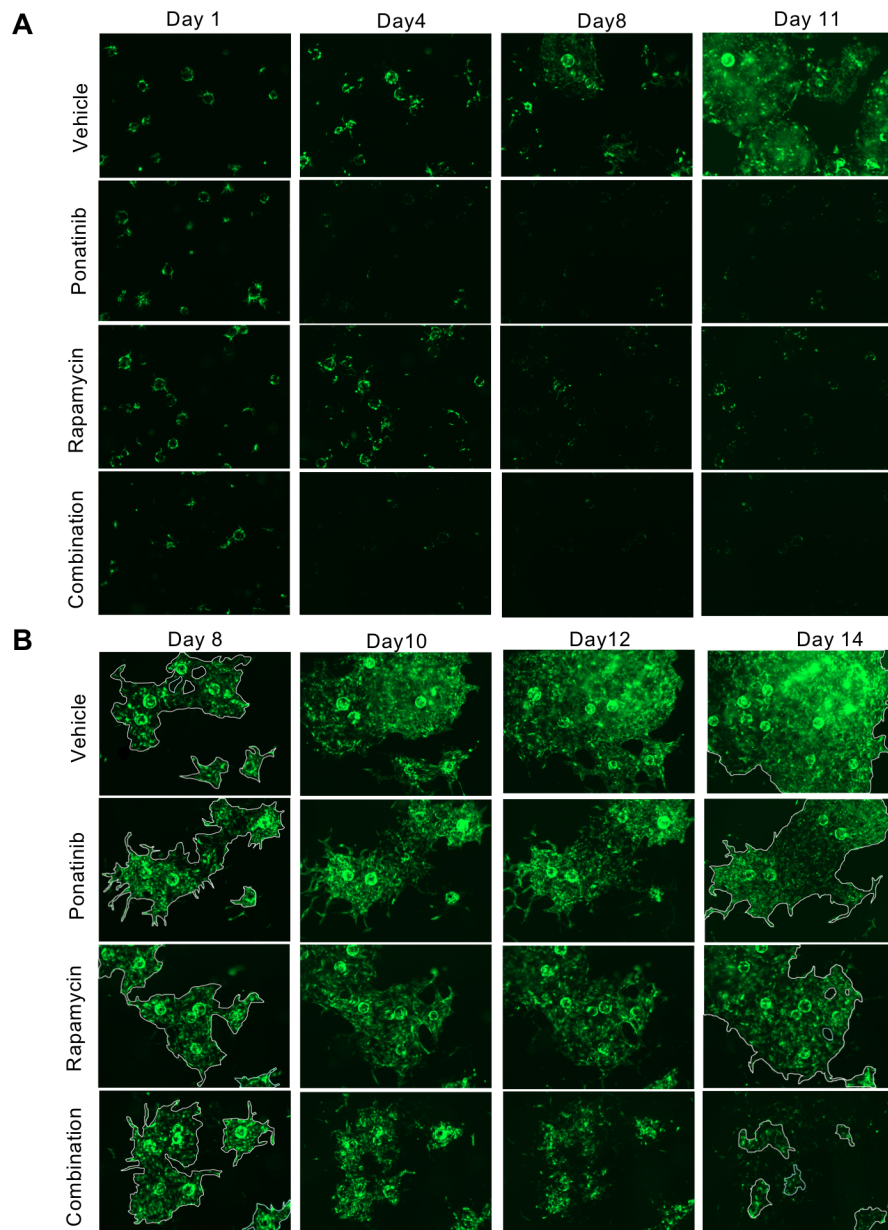
Supplemental figure X. Topical rapamycin treatment prevents VM lesion rebound.

A. Waterfall plot of lesion size change (Day42/Day28). **B.** Lesion weight at Day42. In A and B data expressed as log10 of single value for each lesion, mean shown by horizontal bars, linear mixed model effect (n = 8 mice with 2 lesions/group).



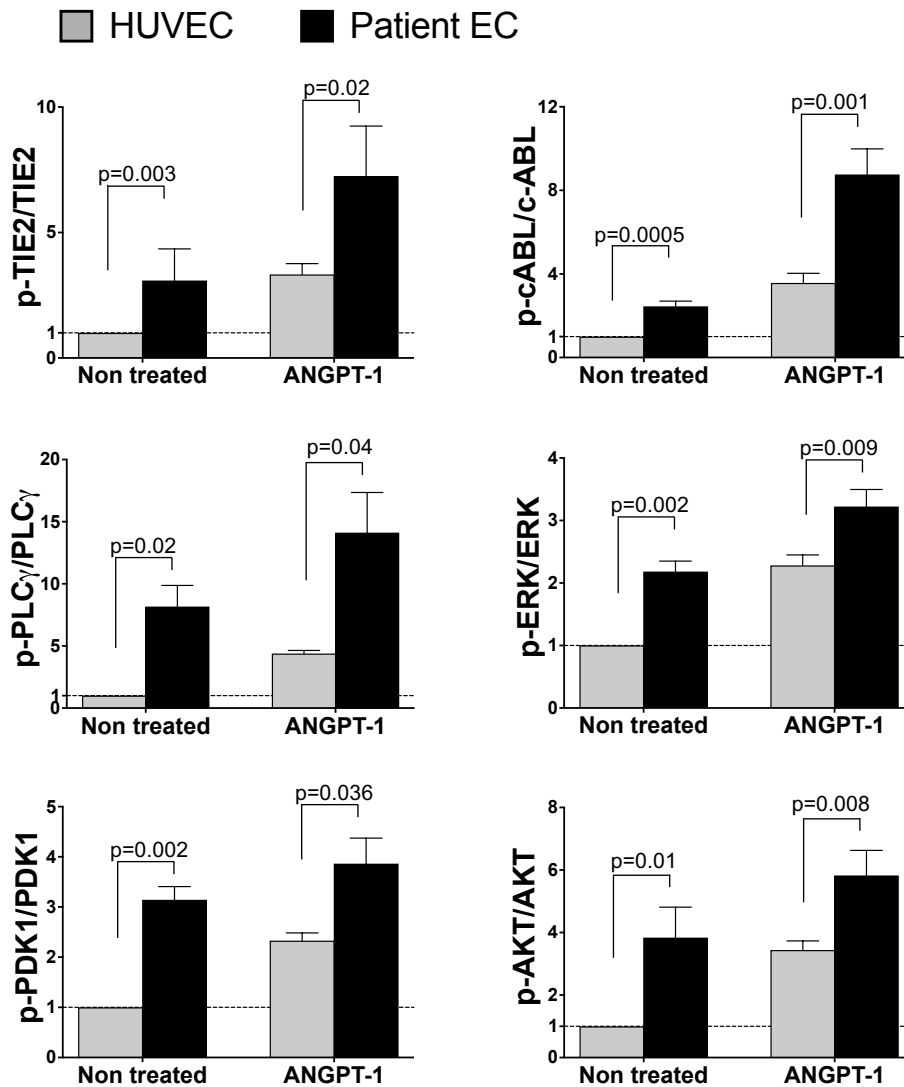
Supplemental figure XI. Combination treatment with Ponatinib and rapamycin increases apoptosis.

A. Representative images of cleaved caspase-3 staining. **B.** Quantification of the ratio of cleaved caspase-3 events (in red) to nuclei (stained with DAPI, in blue). HUVEC-TIE2-L914F cells were treated with DMSO, 300nM Ponatinib, 10nM rapamycin or combination for 72 hours. Data expressed as mean \pm SD (n = 4).



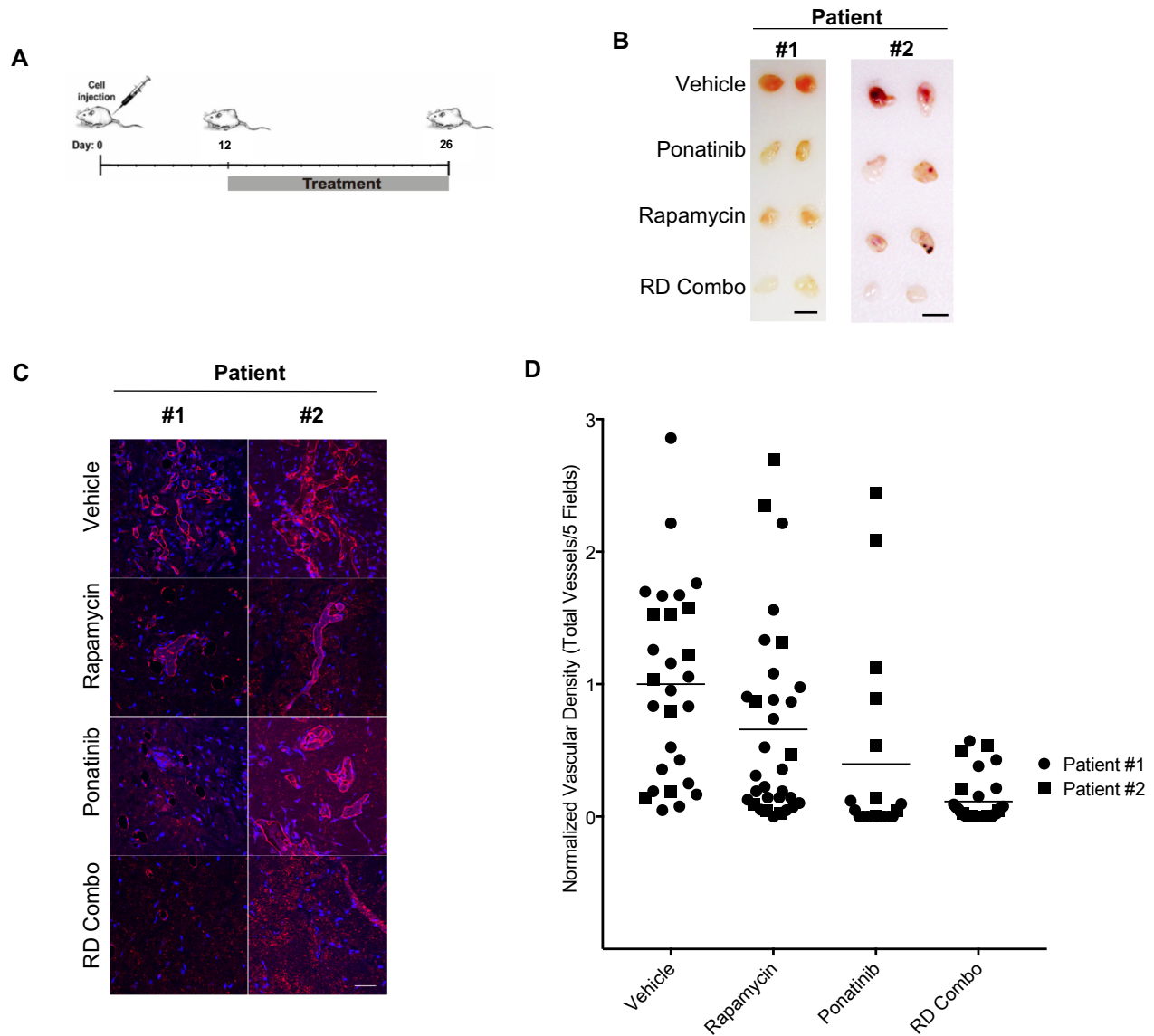
Supplemental figure XII. Combination treatment with Ponatinib and rapamycin reduces vascular area in a 3D fibrin gel assay.

A. Representative 2D images of HUVEC-TIE2-L914F-GFP tube network formation taken on the same field every 3 days from day 1 to 11. **B.** Representative images of HUVEC-TIE2-L914F-GFP tube network regression taken on the same field every other day from day 8 to 14.



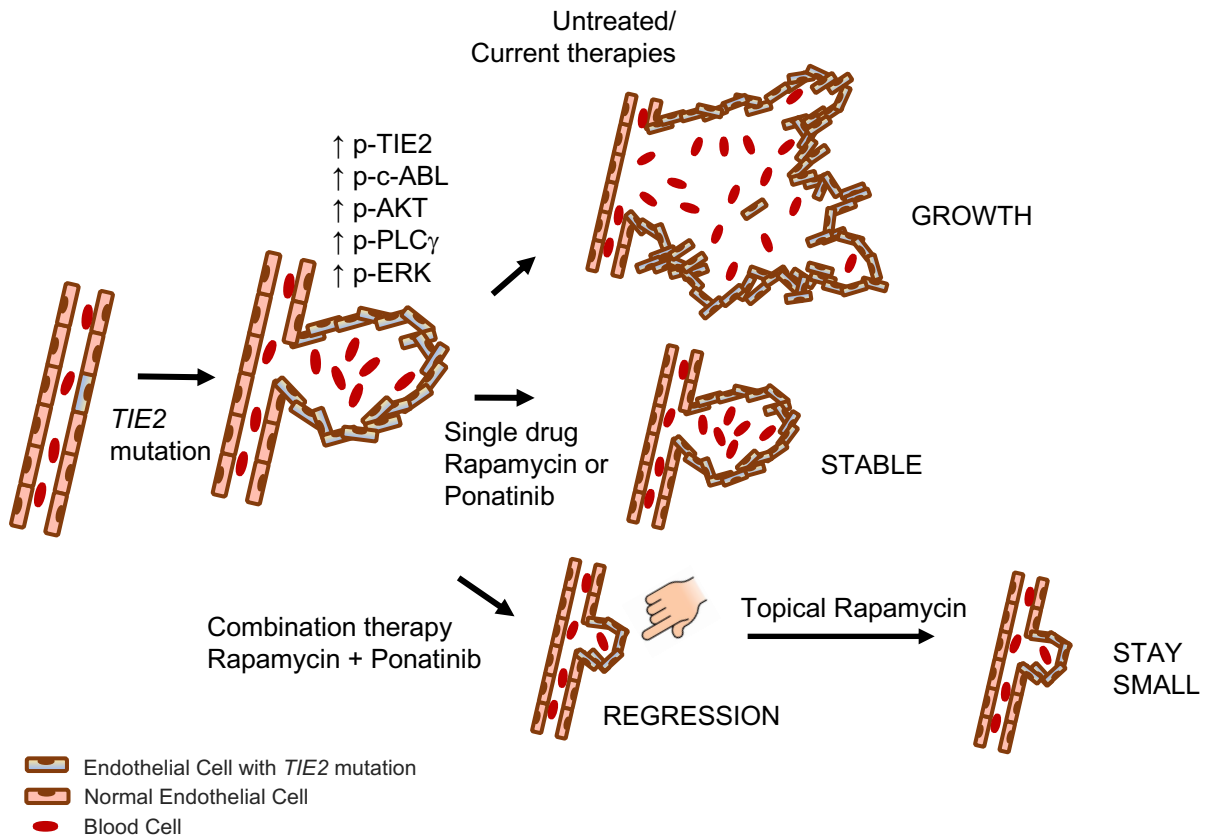
Supplemental figure XIII. Quantification of active signaling pathways in patient-derived VM-EC.

Quantification analysis of immunoblotting of HUVEC and patient EC (patient #1 and #2 VM-EC data are combined) with indicated antibodies (representative immunoblot is Fig.8B). Cells were treated with or without 500nM ANGPT1 for 15 minutes. Data are normalized to HUVEC non treated, Student's t-test (n=3-4).



Supplemental figure XIV. Combination treatment with Ponatinib and rapamycin reduces vascular area in a VM patient-derived xenograft model.

A. VM-EC were injected into mouse at day 0 and treatment was started at day 12 for 14 days. Treatment was daily oral gavage with vehicle, Ponatinib (30mg/kg), rapamycin (2mg/kg) and reduced dose combination (RD Combo, Ponatinib 20mg/kg + rapamycin 1mg/kg). **B.** Representative image of patient (#1 and #2) derived VM-EC xenograft lesions. Scale bar: 1cm. **C.** Representative images of UEA (red) and DAPI (blue) stained sections. Scale bar: 50 μ m. **D.** Quantification of vascular density. Data expressed as normalized single value for each lesion, mean shown by horizontal bars (n = 6-8 mice/group with 2 lesions/mouse). Circle and square represent VM-lesion from patient #1 and patient #2 respectively.



Supplemental figure XV. Schematic model of combination therapy for the treatment of VM.

A *TIE2*-L914F mutation in one or a small subset of EC is sufficient to induce the formation of Venous Malformation (VM). Mutant VM EC show constitutive activation of *TIE2* and downstream AKT and c-ABL (novel finding of this manuscript), and drive lumen enlargement that leads to massive blood vessel expansion. In this manuscript, we show that monotherapy treatment with Rapamycin or Ponatinib results in blood vessel stabilization (no expansion), moreover when Ponatinib and rapamycin are combined a significant regression in VM lesion size occurs. Furthermore, topical rapamycin can prevent VM lesion rebound due to oral drug combination withdrawal.

DRUG NAME (USA)	Average proliferation Inhibition rate (%)			P value (compare L914F with HUVEC)	P value (compare L914F with WT)	Targets
	L914F	NT	WT			
Bortezomib	81.02±0.89	81.03±5.14	69.51±7.04	1.000	0.065	proteasome inhibitor
Enzalutamide	80.92±1.44	82.91±2.91	66.47±9.64	0.346	0.079	androgen receptor antagonist drug
Ixabepilone	79.66±3.72	74.27±3.46	60.18±5.63	0.116	0.004	antimicrotubules
Crizotinib	78.52±3.35	63.84±1.51	64.75±11.63	0.002	0.130	ALK and ROS1 inhibitor
Carfilzomib	76.82±5.78	69.65±10.70	65.03±6.67	0.358	0.061	proteasome inhibitor
Ceritinib	76.61±1.43	12.43±13.48	15.47±17.03	0.004	0.008	ALK inhibitor
Ponatinib	75.54±2.74	26.65±14.27	50.75±12.14	0.008	0.035	tyrosine kinase inhibitor(BCR-Abl)
Omacetaxine mepesuccinate	74.10±2.26	79.78±1.33	67.59±6.99	0.014	0.207	protein translation inhibitor
Cabozantinib	73.71±6.62	32.03±6.09	58.30±5.03	0.000	0.020	multi-targeted RTK inhibitor (c-Met, VEGFR)
Mitoxantrone	73.58±1.67	80.34±3.66	69.91±8.73	0.041	0.522	type II topoisomerase inhibitor
Daunorubicin hydrochloride	70.03±4.09	75.98±5.08	57.27±2.00	0.168	0.007	antimetabolites
Mitomycin	69.37±3.23	69.46±8.38	53.54±7.03	0.986	0.022	chemotherapeutic agents
Topotecan hydrochloride	68.43±3.07	77.50±2.36	63.84±9.29	0.008	0.467	topoisomerase inhibitor
Vandetanib	66.66±5.55	57.75±11.62	48.98±3.14	0.014	0.006	multi-targeted RTK inhibitor (VEGFR, EGFR, RET)
Epirubicin hydrochloride	64.66±1.97	74.39±4.94	54.67±3.51	0.035	0.009	antimetabolites
Doxorubicin hydrochloride	64.48±1.42	73.23±4.36	55.44±3.18	0.034	0.010	antimetabolites
Teniposide	63.88±6.46	60.03±3.71	49.87±10.98	0.414	0.117	chemotherapeutic agent
Dactinomycin	60.39±2.37	66.96±5.62	45.02±6.55	0.135	0.021	inhibit transcription
Plicamycin	60.14±2.17	65.66±4.17	47.75±4.92	0.104	0.015	RNA synthesis inhibitor
Temsirolimus	58.26±9.44	41.50±5.39	31.50±5.07	0.047	0.009	mTOR inhibitor
Bosutinib	57.65±10.30	35.82±5.54	36.20±7.65	0.026	0.030	tyrosine kinase inhibitor (BCR-Abl, Src family kinase)
Belinostat	54.56±4.92	79.38±3.41	37.29±10.31	0.001	0.055	histone deacetylase inhibitor
Siriolimus	53.86±2.78	43.15±2.85	30.27±4.88	0.003	0.001	mTOR inhibitor
Sunitinib	53.00±8.71	34.85±8.76	38.55±11.15	0.044	0.130	multi-targeted RTK inhibitor (VEGFR, PDGFR)
Gemcitabine hydrochloride	52.68±2.66	50.73±8.68	37.43±11.02	0.731	0.093	DNA synthesis;
Everolimus	50.48±4.75	39.76±3.54	28.02±3.93	0.038	0.002	mTOR inhibitor;
Sorafenib	49.65±15.29	13.24±7.39	8.77±8.18	0.020	0.013	multi-targeted RTK inhibitor (VEGFR and PDGFR)
Bleomycin sulfate	49.04±3.45	50.88±6.71	29.04±2.53	0.693	0.000	antibiotics
Thioguanine	47.63±5.54	13.78±5.10	30.81±5.81	0.000	0.011	antimetabolites
Valrubicin	45.35±21.71	-4.92±7.16	2.82±4.06	0.022	0.040	antibiotic
Pazopanib hydrochloride	45.34±21.95	4.01±24.21	31.78±22.26	0.071	0.481	multi-targeted RTK inhibitor (VEGFR, PDGFR, FGFR, c-Kit and c-Fms)
Clofarabine	44.23±1.93	55.78±7.52	35.23±11.44	0.073	0.267	antimetabolites
Paclitaxel	42.90±4.11	47.99±3.25	41.64±4.36	0.146	0.727	microtubule inhibitor
Vorinostat	42.80±2.50	72.11±6.08	30.92±14.92	0.002	0.263	Histone deacetylase inhibitors
Azacitidine	42.64±4.84	44.27±6.66	31.51±3.90	0.744	0.022	chemotherapeutic agents
Afatinib	41.38±31.06	20.01±5.26	13.07±2.30	0.321	0.212	multi-targeted RTK inhibitor (EGFR, HER2)
Dabrafenib mesylate	40.95±5.81	22.13±9.95	-6.26±4.13	0.038	0.000	BRAF inhibitor
Triethylenemelamine	40.60±5.76	46.10±7.11	20.73±6.02	0.341	0.006	chemotherapeutic agent
Cladribine	40.23±3.53	57.01±6.49	33.35±11.53	0.013	0.386	antimetabolites
Trametinib	40.22±4.19	34.72±1.51	-0.64±5.09	0.104	0.000	MEK inhibitor
Oxaliplatin	39.55±2.37	25.39±2.42	13.52±5.20	0.000	0.001	chemotherapeutic agent
Vinblastine sulfate	35.39±1.69	53.78±2.67	43.02±4.33	0.000	0.048	microtubule inhibitor
Regorafenib	35.36±3.79	56.71±4.94	34.68±9.16	0.001	0.910	multi-targeted RTK inhibitor (VEGFR2, TIE2)
Vinorelbine tartrate	35.26±3.43	51.59±2.84	36.04±5.83	0.001	0.850	microtubule inhibitor
Etoposide	34.62±3.82	47.96±5.14	26.52±7.47	0.013	0.162	topoisomerase inhibitor
Pralatrexate	34.60±34.53	-2.94±0.94	-13.51±5.14	0.160	0.095	folate analogue metabolic inhibitor
Vincristine sulfate	32.81±4.16	49.75±2.60	29.41±9.93	0.002	0.613	microtubule inhibitor
Fluorouracil	32.67±3.70	20.48±6.08	16.43±3.45	0.032	0.001	antimetabolites
Cytarabine hydrochloride	30.30±4.96	42.88±12.84	27.99±9.66	0.191	0.728	chemotherapeutic agents
Romidepsin	29.66±3.66	50.89±2.44	39.07±7.70	0.000	0.124	Histone deacetylase inhibitors
Axitinib	28.13±12.90	18.51±6.09	2.30±11.05	0.304	0.040	multi-targeted RTK inhibitor (VEGFR, c-KIT, PDGFR)
Gefitinib	26.69±5.05	11.93±4.12	19.20±19.54	0.008	0.561	EGFR inhibitor
Ibrutinib	24.52±8.83	31.64±16.99	25.81±10.98	0.551	0.880	Bruton's tyrosine kinase
Idelalisib	23.39±3.19	23.75±5.89	36.19±2.62	0.929	0.002	phosphoinositide 3-kinase inhibitor
Irinotecan hydrochloride	22.26±3.10	44.02±8.12	19.37±2.33	0.013	0.247	topoisomerase inhibitor
Mechlorethamine hydrochloride	21.76±2.99	41.12±8.77	14.22±6.46	0.026	0.137	chemotherapeutic agents
Cabazitaxel	21.15±3.98	40.06±6.34	32.37±5.79	0.007	0.037	microtubule inhibitor
Floxuridine	19.64±3.56	23.25±2.06	10.72±2.36	0.192	0.014	antimetabolites
Docetaxel	18.42±7.10	38.82±6.01	31.54±3.95	0.009	0.041	microtubule inhibitor
Uracil mustard	17.47±3.41	18.80±8.40	6.77±3.14	0.811	0.007	chemotherapeutic agents
Nilotinib	13.11±4.53	-7.48±8.48	-9.36±7.28	0.028	0.016	tyrosine kinase inhibitor (BCR-Abl, c-KIT, Lck)
Lomustine	12.00±2.39	12.58±5.16	11.37±5.21	0.869	0.856	chemotherapeutic agents
Olaparib	11.51±2.51	16.80±7.5	10.97±2.08	0.317	0.782	chemotherapeutic agent
Mercaptopurine	10.90±6.64	6.10±5.02	0.45±1.76	0.360	0.068	immunosuppressive drug
Chlorambucil	10.85±4.46	22.00±1.90	3.69±3.26	0.016	0.070	chemotherapeutic agents
Dexrazoxane	10.82±4.08	13.37±6.52	5.76±6.04	0.589	0.281	cardioprotective agent
Erlotinib hydrochloride	10.67±13.50	35.28±16.84	25.46±13.32	0.098	0.226	antimetabolites
Tamoxifen citrate	10.45±5.96	24.32±19.11	37.26±11.75	0.304	0.020	selective estrogen-receptor modulator
Thiotepa	10.25±7.23	21.58±4.76	8.06±1.92	0.071	0.642	chemotherapeutic agents
Pipobroman	10.05±1.23	15.75±6.46	3.55±4.34	0.225	0.076	chemotherapeutic agents/alkylating agent
Melphalan hydrochloride	9.53±3.93	11.09±5.24	-1.25±2.16	0.694	0.010	alkylating agents
Decitabine	8.76±2.58	3.11±3.23	-1.12±5.45	0.058	0.043	DNA methyltransferase inhibitor
Raloxifene	7.46±1.71	9.41±7.33	28.24±26.13	0.681	0.262	selective estrogen receptor modulator (SERM)
Carmustine	7.11±6.51	11.20±3.21	3.32±2.51	0.380	0.401	chemotherapeutic agents
Exemestane	6.56±2.99	5.08±3.26	-4.29±2.60	0.585	0.003	aromatase inhibitors
Lapatinib	6.44±5.74	-2.48±5.78	-3.81±7.41	0.107	0.110	multi-targeted RTK inhibitor (HER2, EGFR)
Letrozole	6.07±3.14	4.31±6.48	-0.85±5.95	0.693	0.141	Aromatase inhibitors
Dasatinib	6.05±14.11	18.57±13.42	16.99±9.69	0.308	0.316	multi- BCR/Abl and Src family tyrosine kinase inhibitor
Procabazine hydrochloride	6.02±7.28	0.84±5.66	-3.53±1.96	0.370	0.105	chemotherapeutic agents
Perifoxa	5.99±3.13	3.15±4.91	-2.43±2.55	0.436	0.012	immunostimulant
Celecoxib	5.55±4.73	0.37±5.65	-10.16±5.65	0.270	0.011	COX-2 selective nonsteroidal anti-inflammatory drug
Abiraterone	5.33±9.30	-6.50±4.67	-7.15±1.25	0.114	0.102	antiandrogen activity
Pemetrexed disodium salt	5.13±3.08	2.48±4.32	-2.57±4.77	0.424	0.064	chemotherapy drugs called folate antimetabolites
Mitotane	4.55±2.29	1.39±4.88	-0.12±2.25	0.365	0.045	antimetabolites
Ifosfamide	4.47±5.64	-3.81±1.30	-0.66±3.83	0.081	0.247	chemotherapeutic agents

Lenalidomide	4.46±2.50	1.27±8.73	-2.09±4.04	0.580	0.063	anti-tumor effect, inhibition of angiogenesis, and immunomodulatory role
Anastrozole	3.95±4.02	4.23±8.05	-1.07±4.15	0.960	0.183	aromatase inhibitors
Fulvestrant	3.89±4.72	-4.95±2.87	-2.52±8.38	0.040	0.304	estrogen receptor antagonist
Idarubicin hydrochloride	3.36±2.99	1.79±6.96	-4.82±3.36	0.737	0.020	antitumor antibiotics.
Nelarabine	3.00±3.31	4.75±5.71	-0.28±1.34	0.667	0.188	chemotherapeutic agents
Megestrol acetate	2.95±4.32	1.49±4.47	-7.37±3.75	0.700	0.021	potent agonist of the progesterone receptor
Cyclophosphamide	2.88±5.30	-1.06±4.30	-4.00±3.45	0.357	0.117	chemotherapeutic agents
Imiquimod	2.68±3.32	-0.75±3.89	-3.32±4.11	0.290	0.099	immune response modifier (IRM)
Bendamustine hydrochloride	2.12±3.14	3.19±5.22	-0.61±2.47	0.774	0.284	chemotherapeutic agents/alkylating agent
Imatinib	1.90±4.30	12.44±23.61	-5.42±4.44	0.499	0.086	multi-targeted RTK inhibitor (BCR-Abl, c-KIT, PDGFR)
Vismodegib	1.57±4.46	-1.48±5.81	-9.97±2.25	0.499	0.013	antagonist of the smoothened receptor (SMO)
Carboplatin	1.26±2.89	3.77±1.74	-3.94±2.60	0.255	0.060	chemotherapeutic agent
Fludarabine phosphate	1.21±1.08	0.14±5.94	-2.30±3.90	0.778	0.218	chemotherapeutic agents
Cisplatin	1.15±2.87	-4.42±4.54	-6.87±5.51	0.278	0.158	chemotherapeutic agents
Capecitabine	1.06±7.33	0.47±5.83	-1.49±3.55	0.876	0.326	chemotherapeutic agents
Vemurafenib	0.70±3.13	-8.56±2.96	-4.40±5.67	0.060	0.230	B-Raf inhibitor
Amifostine	0.66±4.19	-8.91±7.17	-11.51±3.99	0.157	0.057	cytoprotective adjuvant
Busulfan	0.26±1.91	1.68±2.47	0.46±3.24	0.560	0.940	chemotherapeutic agents
Tretinoin	0.11±4.76	-3.57±2.74	-7.14±6.55	0.257	0.166	retinoic acid receptors agonist
Methoxsalen	-0.04±1.91	-1.93±2.06	-1.69±3.24	0.289	0.482	furanocoumarins
Allopurinol	-0.18±4.76	1.79±4.53	-1.38±2.80	0.621	0.723	antimetabolites
Arsenic trioxide	-0.26±2.86	1.49±3.99	2.81±4.60	0.562	0.371	unclear
Zoledronic acid	-0.37±4.93	-8.23±9.55	-11.71±5.29	0.267	0.035	anti-bone-resorption
Streptozocin	-0.95±6.61	-5.23±5.62	-5.84±6.97	0.427	0.412	chemotherapeutic agents
Temozolomide	-1.03±2.84	3.01±3.34	0.12±3.03	0.162	0.649	chemotherapeutic agents
Aminolevulinic acid hydrochloride	-1.31±5.00	3.76±6.35	-3.60±4.41	0.321	0.575	porphyrin synthesis inhibitor
Pomalidomide	-1.48±5.61	5.37±5.50	-4.53±2.86	0.182	0.445	inhibition of angiogenesis, and immunomodulatory role
Thalidomide	-2.35±5.55	-1.60±8.12	-5.38±2.54	0.900	0.437	immunomodulatory drug
Estramustine phosphate sodium	-2.46±3.51	-4.58±1.90	-3.54±11.35	0.403	0.883	antimicrotubule
Pentostatin	-2.59±3.70	-3.07±3.80	-5.53±4.48	0.880	0.416	chemotherapeutic agents
Hydroxyurea	-2.83±3.89	-2.21±6.97	-1.53±1.92	0.898	0.630	antimetabolites
Methotrexate	-2.85±13.31	-3.40±8.89	-7.58±6.88	0.955	0.610	antimetabolites
Altretamine	-3.57±4.87	2.67±4.32	-0.88±4.13	0.120	0.493	chemotherapeutic agents
Dacarbazine	-3.94±2.38	1.88±5.20	-3.57±1.78	0.150	0.839	alkylating agents

Supplementary Table I. Cell-based drug screening assay results.

This table includes proliferation inhibition rates of 119 FDA approved drugs at 20 μ M in HUVEC-TIE2-L914F, -TIE2-wild type (WT) and non transfected (NT).

Compounds	IC50 (μ M)			Targets
	L914F	WT	NT	
Sirolimus	<0.03	<0.03	<0.03	mTOR inhibitor
Temsirolimus	<0.03	<0.03	<0.03	
Everolimus	<0.03	<0.03	<0.03	
Ponatinib	0.42±0.03	0.89±0.24	1.26±0.42	BCR-Abl inhibitor
Bosutinib	3.54±1.14	4.1±0.68	5.16±1.85	
Nilotinib	3.61±0.03	4.98±0.90	6.39±1.18	
Cabozantinib	3.06±0.27	2.89±1.16	1.35±0.20	multi-targeted RTK inhibitor(c-Met, VEGFR)
Vandetanib	>10	5.63±0.24	6.20±0.95	multi-targeted RTK inhibitor (VEGFR,EGFR, RET)
Sorafenib	>10	>10	6.84±2.23	multi-targeted RTK inhibitor(VEGFR, PDGFR)
Ceritinib	9.03±1.38	8.66±2.98	8.13±2.65	ALK inhibitor
Dabrafenib mesylate	>10	>10	>10	BRAF inhibitor

Supplementary Table II. List of candidate drugs and IC50 values.

This table includes IC50 values of 11 candidate drugs in HUVEC-TIE2-L914F, -TIE2-wild type (WT) and non transfected (NT), in a 6 dose dilution (from 10 to 0.03 μ M) assay. IC50 of several drugs could not be confirmed as the value were out of the concentration range tested.

Rapamycin	Ponatinib			Nilotinib			Bosutinib		
	L914F	WT	NT	L914F	WT	NT	L914F	WT	NT
Combination Index	0.67±0.26	0.74±0.32	0.89±0.24	0.8±0.28	0.58±0.15	0.71±0.27	1.49±0.31	1.72±0.41	1.47±0.41

Supplementary Table III. Combination index (CI) values.

This table includes Combination Index (CI) value of three ABL kinase inhibitors combined with rapamycin in HUVEC-TIE2-L914F, -TIE2-wild type (WT) and non transfected (NT).

Major Resources Tables

Animals (in vivo studies)

Species	Vendor or Source	Background Strain	Sex
mouse	Envigo	Nu/nu	Male

Note: Nude mice are only acting as a host for the grafted HUVEC-TIE2-L914F and for patient-derived cells, using male mice that do not have the hormone cycling is the best strategy to study vasculogenesis.

Drugs

Compound name	Vendor or Source	Catalog number
Drug library for in vitro screen	NCI (DTP program) plated compounds	
Ponatinib	LC Laboratory	P-7022
Bosutinib	NCI (DTP program) vialled compound	
Nilotinib	NCI (DTP program) vialled compound	
rapamycin	LC Laboratory	R-5000

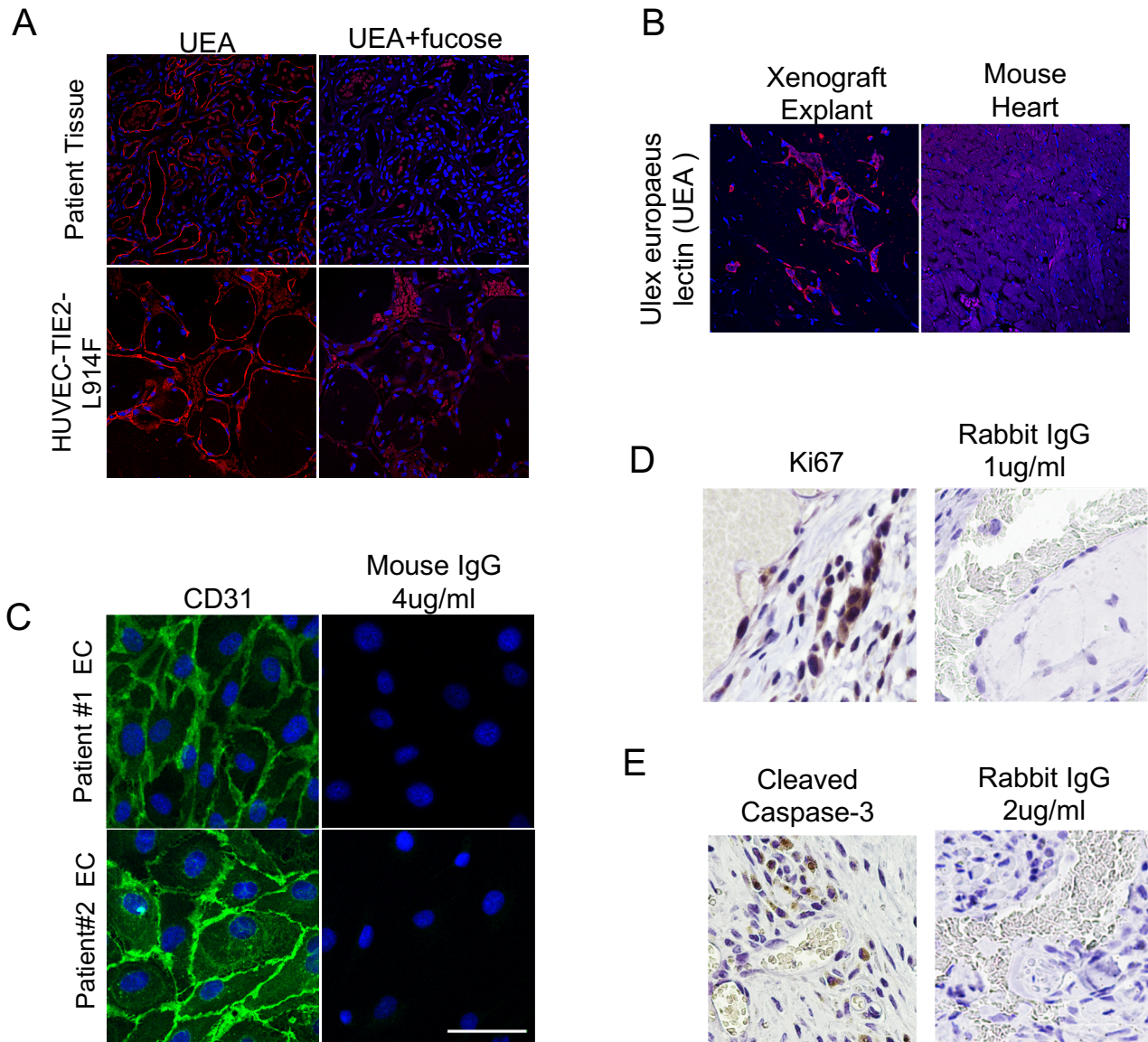
Antibodies

Target antigen	Vendor or Source	Catalog #	Working concentration	Lot # (preferred but not required)
p-cABL	Cell Signaling	2868	0.4 µg/ml	6
c-ABL	Cell Signaling	2862	1.5 µg/ml	16
ARG	Novus Biological	NBP1-18875	1 µg/ml	A1
p-TIE2	Cell Signaling	4221	0.002 µg/ml	4
TIE2	Cell Signaling	7403	0.175 µg/ml	1
p-AKT (Ser 473)	Cell Signaling	4060	0.05 µg/ml	23
p-AKT (Thr 308)	Cell Signaling	2965	0.35 µg/ml	18
AKT	Cell Signaling	9272	0.04 µg/ml	27
p-ERK	Cell Signaling	4370	0.17 µg/ml	17
ERK	Cell Signaling	9102	0.02 µg/ml	27
p-PLCg	Cell Signaling	2821	0.08 µg/ml	9
PLCg	Cell Signaling	2822	0.06 µg/ml	5
p-PDK1	Cell Signaling	3061	0.008 µg/ml	3
PDK1	Cell Signaling	3062	0.1 µg/ml	12
Tubulin	Sigma	T9026	10 µg/ml	083M4847V
β-Actin	Sigma	A5441	1 µg/ml	014M4759
Cleaved Caspase-3	Cell Signaling	9661S	2 µg/ml	43
Ki-67	Abcam	ab66155	1 µg/ml	GR134821-14
UEA	VectorLabs	B-1065	20 µg/ml	Z0806
CD31	Dako	M082329-2	2 µg/ml	20036220

Cultured Cells

Name	Vendor or Source	Sex (F, M, or unknown)
HUVEC-TIE2-L914F	Mikka Vikkula's laboratory	unknown
HUVEC-TIE2-WT	Mikka Vikkula's laboratory	unknown
HUVEC-NT	Mikka Vikkula's laboratory	unknown
VM patient derived endothelial cells (Patient#1 and Patient#2)	VM patient lesional tissue	Male and Female

Immunostaining Negative Controls



Immunostaining Negative Controls.

A. Immunofluorescent staining for Ulex europaeus agglutinin I (UEA) in red and DAPI in blue (left). We stained vascular anomaly patient tissue (top) and HUVEC-TIE2-L914F-derived VM lesion in mouse (bottom). Fucose was added as a negative control as it binds to UEA (right).

B. Immunofluorescent staining for Ulex europaeus agglutinin I (UEA) in red and DAPI in blue. We stained patient-derived VM-EC xenograft explant (left) and mouse heart (right) to show specificity of UEA for human-derived endothelium.

C. Immunofluorescent staining for CD31 in green and DAPI in blue (left) or mouse IgG in green and DAPI (right). We stained patient-derived VM-EC monolayer, patient#1 (top), patient#2 (bottom).

D. Immunohistochemical staining for Ki-67 (left) and rabbit IgG (right) on HUVEC-TIE2-L914F-derived VM lesion in mouse.

E. Immunohistochemical staining for Cleaved Caspase-3 (left) and rabbit IgG (right) on HUVEC-TIE2-L914F-derived VM lesion in mouse.